

1 **A global analysis approach for investigating structural resilience in urban drainage**  
2 **systems**

3 **Seith N. Mugume<sup>a</sup>, Diego E. Gomez, Guangtao Fu, Raziye Farmani, David Butler**

4 <sup>a</sup> Centre for Water Systems, College of Engineering, Mathematics and Physical Sciences, University of Exeter,  
5 North Park Road, Exeter, EX4 4QF, United Kingdom; Tel: +44 (0)1392 723600, E-mail:  
6 [snm205@exeter.ac.uk](mailto:snm205@exeter.ac.uk)

**Abstract:** Building resilience in urban drainage systems requires consideration of a wide range of threats that contribute to urban flooding. Existing hydraulic reliability based approaches have been focused on quantifying functional failure caused by extreme rainfall or increase in dry weather flows that lead to hydraulic overloading of the system. Such approaches however, do not fully explore the full system failure scenario space due to exclusion of crucial threats such as equipment malfunction, pipe collapse and blockage that can also lead to urban flooding. In this research, a new analytical approach based on global resilience analysis is investigated and applied to systematically evaluate the performance of an urban drainage system when subjected to a wide range of structural failure scenarios resulting from random cumulative link failure. Link failure envelopes, which represent the resulting loss of system functionality (impacts) are determined by computing the upper and lower limits of the simulation results for total flood volume (failure magnitude) and average flood duration (failure duration) at each link failure level. A new resilience index that combines the failure magnitude and duration into a single metric is applied to quantify system residual functionality at each considered link failure level. With this approach, resilience has been tested and characterized for an existing urban drainage system in Kampala city, Uganda. In addition, the effectiveness of potential adaptation strategies in enhancing its resilience to cumulative link failure has been tested.

**Keywords:** failure envelopes, flexibility, redundancy, resilience, structural failure, urban water management

7

8

## 9 Nomenclature

10	$rs_i$	random link failure sequence
11	$ns_i$	random failure sequences for the existing system
12	$cs_i$	random failure sequences for the centralised storage strategy
13	$ds_i$	random failure sequences for the distributed storage strategy
14	$N$	total number of links
15	$n$	Manning's roughness coefficient
16	$t_f$	mean duration of nodal flooding
17	$t_r$	total rainfall event duration
18	$Res_o$	operational resilience index
19	$T$	rainfall return period in years
20	$V_{TF}$	total flood volume
21	$V_{TI}$	total inflow volume
22	$\mu$	mean
23	$\sigma$	standard deviation
24		

## 1. Introduction

25 Recent natural and manmade catastrophic events that have led to extreme flooding in various  
26 cities worldwide have underscored the need to build resilience into existing urban drainage  
27 and flood management systems as a key strategy to minimise the resulting flooding impacts  
28 and consequences (Djordjević et al., 2011; Park et al., 2013). Urban drainage system flooding  
29 is not only caused by *external* climate-related and urbanisation threats such as extreme  
30 rainfall and increasing urbanisation but also *internal* system threats for example equipment  
31 malfunction, sewer collapse and blockages (Kellagher et al., 2009; Mugume et al., 2014; Ryu  
32 and Butler, 2008; Ten Veldhuis, 2010). System or component failures can either be abrupt  
33 (unexpected) shocks for example pump or sensor failure or chronic pressures such as asset  
34 aging and long term asset decay or sewer sedimentation. The impact of such failures, either  
35 singly or in combination on existing urban drainage infrastructure could significantly reduce  
36 the expected **flood** protection service levels in cities and lead to negative consequences such  
37 as loss of lives, damage to properties and critical infrastructure (Djordjević et al., 2011;  
38 IPCC, 2014; Ryu and Butler, 2008; Ten Veldhuis, 2010).

39 Consequently, the need to build resilience in urban drainage systems (UDSs) is increasingly  
40 recognised as vital to enhance their ability to maintain acceptable flood protection service  
41 levels in cities that they serve and to minimise the resulting flooding consequences during  
42 unexpected or exceptional loading conditions that lead to system failure (Butler et al., 2014;  
43 Djordjević et al., 2011). Although the application of concept of *resilience* to infrastructure  
44 systems is a recent development, there is an extensive literature on definitions and  
45 interpretation of resilience, much of which has come from the ecological systems academic  
46 community (Butler et al., 2014; Park et al., 2013). Ecological system resilience is interpreted  
47 as a measure of *system integrity* and is defined as a system's ability to maintain its basic  
48 structure and patterns of behaviour (i.e. to persist) through absorbing shocks or disturbances

49 under dynamic (non-equilibrium) conditions (Holling, 1996). In contrast to ecological  
 50 systems, engineering systems are product of intentional human invention and are designed to  
 51 provide continued (uninterrupted) services to society in an efficient manner (Blackmore and  
 52 Plant, 2008; Holling, 1996; Park et al., 2013). Engineering system resilience is therefore  
 53 interpreted differently from ecological resilience and focuses on ensuring *continuity and*  
 54 *efficiency of system function* during and after failure (Butler et al., 2014; Lansey, 2012)

55 In the context of urban drainage, current design and rehabilitation approaches tend to focus  
 56 on prevention of hydraulic (functional) failures resulting from a specified design storm of a  
 57 given frequency (i.e. return period). The design storm return period determines the flood  
 58 protection level provided by the system (Butler and Davies, 2011). However, such hydraulic  
 59 reliability-based design approaches place significant emphasis on *identifying* and *quantifying*  
 60 the probability of occurrence of extreme rainfall and *minimising* the probability of the  
 61 resulting hydraulic failures i.e. *the fail-safe approach* (Ryu and Butler, 2008; Thorndahl and  
 62 Willems, 2008). However, such approaches fail to consider other causes of failure for  
 63 example structural or component failures (Table 1) which also lead to flooding (e.g.  
 64 Kellagher et al., 2009; Mugume et al., 2014; Ten Veldhuis, 2010).

65 **Table 1:** Failure modes in urban drainage systems

<b>Failure mode</b>	<b>Description</b>	<b>Examples/Causes</b>
Functional failure	Hydraulic overloading due to changes in inflows leading to failure e.g. overflow operation, surcharging and surface flooding	Increase in dry weather flows, extreme rainfall events, excessive infiltration
Structural failure	Malfunctioning of single or multiple components in the system such as pumps, tanks or pipes leading to the inability of the failed component to deliver its desired function in full or in part	Pipe collapse, blockages, sediment deposition, solid waste, pump failure, rising main failure

66

67 Furthermore, it is argued that the direct application of reliability-based approaches for  
 68 evaluation of structural failures in UDSs could be insufficient mainly because causes and

69 mechanisms of failure are largely unknown and difficult to quantify (Ana and Bauwens,  
70 2010; Kellagher et al., 2009; Park et al., 2013; Ten Veldhuis, 2010). It is therefore important  
71 to develop new approaches that seek to ensure that UDSs are designed to not only be reliable  
72 during *normal* (standard) loading conditions but also to be resilient to *unexpected*  
73 (exceptional) conditions i.e. *the safe-fail approach* (e.g. Butler et al., 2014; Mugume et al.,  
74 2014). In this study, the definition and interpretation of resilience in engineering systems is  
75 pursued. Resilience is formally defined based on recent work on ‘Safe and SuRe’ Water  
76 Management as the “*the degree to which the system minimises level of service*  
77 *failure magnitude and duration over its design life when subject to exceptional conditions*”  
78 (Butler et al., 2014). Exceptional conditions refer to uncertain threats or disturbances that lead  
79 to system failure for example climate change induced extreme rainfall events, sewer collapse  
80 or blockage. Based on this definition, the goal of resilience is therefore to maintain acceptable  
81 functionality levels (by withstanding service failure) and rapidly recover from failure once it  
82 occurs (Butler et al., 2014; Lansey, 2012; Park et al., 2013).

83 Resilience is further classified into two broad categories: a) *general (attribute-based)*  
84 *resilience* which refers to the state of the system that enables it to limit failure duration and  
85 magnitude to *any threat* (i.e. all hazards including unknowns) and b) *specified (performance-*  
86 *based)* resilience which refers to the agreed performance of the system in limiting failure  
87 magnitude and duration to a *given (known) threat* (Butler et al., 2014; Scholz et al., 2011).  
88 Reliability on the other hand is defined as *the degree to which the system minimises the level*  
89 *of service failure frequency over its design life when subject to standard loading* (Butler et  
90 al., 2014). Intuitively, it is argued that reliability and resilience are related with the latter  
91 extending and building on the former. It is consequently postulated that if resilience builds on  
92 reliability, by improving the former, the latter can also be improved (Butler et al., 2014).

93 Taking the UK water sector as an example, recent studies have proposed range of strategies  
94 or options for building resilience in UDSs (Cabinet Office, 2011; CIRIA, 2014; McBain et al.,  
95 2010). These strategies generally seek to enhance inbuilt system properties or attributes such  
96 as *redundancy* and *flexibility* during design, retrofit or rehabilitation so as to influence the  
97 ability of the system to withstand the level of service failure and to rapidly recover from  
98 failure once it occurs (Hassler and Kohler, 2014; Vugrin et al., 2011). Redundancy is defined  
99 as the degree of overlapping function in a system that permits the system to change in order  
100 to allow vital functions to continue while formerly redundant elements take on new functions  
101 (Hassler and Kohler, 2014). In UDSs, redundancy is enhanced by introducing multiple  
102 elements (components) providing similar functions for example storage tanks or parallel  
103 pipes, in order to minimize failure propagation through the system or to enable operations to  
104 be diverted to alternative parts of the system during exceptional loading conditions (Cabinet  
105 Office, 2011; Mugume et al., 2014). Flexibility on the other hand is defined as the inbuilt  
106 system capability to adjust or reconfigure so as to maintain acceptable performance levels  
107 when subject to multiple (varying) loading conditions (Gersonius et al., 2013; Vugrin et al.,  
108 2011). It can be achieved in UDSs, for example, by designing in future proofing options  
109 (Gersonius et al., 2013), use of distributed (decentralized) or modular elements for example  
110 distributed storage tanks, rainwater harvesting systems, roof disconnection and use of  
111 designed multifunctional urban spaces such as car parks, playgrounds or roads (Mugume et  
112 al., 2014).

113 However, the operationalisation of resilience in urban drainage and flood management is still  
114 constrained by lack of guidelines, standards, and suitable quantitative evaluation methods  
115 (Butler et al., 2014; Ofwat, 2012; Park et al., 2013). In water distribution systems, a number  
116 of recent studies have investigated both *component (structural)* and *hydraulic* reliability  
117 when subject to stresses such as demand variations, single pipe failure and changes in pipe

118 roughness (Atkinson et al., 2014; Trifunovic, 2012). In urban drainage systems however,  
119 most quantitative studies tend to focus on investigating *hydraulic reliability* which only  
120 considers *functional failures* such as occurrence of extreme rainfall or increasing dry weather  
121 flows (Sun et al., 2011; Thorndahl and Willems, 2008). The main short coming of such  
122 approaches is that the full system failure scenario space that includes other causes of surface  
123 flooding such as equipment failure, sewer collapse and blockage is not explored.

124 It is recognised that different threats or combinations of threats such as extreme rainfall or  
125 sewer failure could lead to the same failed state (i.e. surface flooding). Therefore, by only  
126 considering a narrow range of hydraulic failures, current approaches take a limited view of  
127 *functional resilience* with no due consideration given to *structural resilience*. Further  
128 research is needed to develop new quantitative approaches that explicitly consider all possible  
129 failure scenarios in order to holistically evaluate resilience in UDSs (Butler et al., 2014;  
130 Kellagher et al., 2009; Ofwat, 2012; Ten Veldhuis, 2010).

131 In this study, a new global resilience analysis approach is developed, that shifts the object of  
132 analysis from the threats themselves to explicit consideration of system performance (i.e.  
133 failed states) when subject to large number of failure scenarios (Johansson, 2010). Global  
134 resilience analysis has been carried out by evaluating the effect of a wide range of  
135 progressive structural failure scenarios in various systems such as water distribution systems  
136 and electrical power systems (Johansson, 2010). The global resilience analysis (GRA)  
137 methodology is extended to investigate the effect of random cumulative link (sewer) failure  
138 scenarios on the performance of an UDS. The methodology is then applied to test the effect  
139 of implementing two potential adaptation strategies that is; introducing a large centralised  
140 detention pond or use of spatially distributed storage tanks) on minimizing loss of  
141 functionality during the considered structural failure scenarios.

142 The key strengths of the developed GRA method is that emphasis is shifted from accurate  
143 quantification of the probability of occurrence of sewer failures (e.g. Egger et al., 2013), to  
144 evaluating the effect of different sewer failures modes and extent, irrespective of their  
145 occurrence probability, on the ability of an UDS to minimise the resulting flooding impacts  
146 (e.g. Kellagher et al., 2009).

147 Link failure envelopes, which show the upper and lower limits (bounds) of the resulting loss  
148 of functionality for each considered link failure level are determined based on the hydraulic  
149 simulation results from 49,200 scenarios. The failure envelopes reflect vital system resilience  
150 properties that determine the resulting loss of functionality when the system is subjected to  
151 increasing failure levels. Finally, a new resilience index,  $Res_o$  that quantifies system residual  
152 functionality as a function of failure magnitude and duration is computed at each failure level  
153 for both the existing system and for the tested adaptation strategies.

## 2. Methods

### 154 2.1 Global resilience analysis (GRA) approach

155 Global resilience analysis is applied to characterise the performance of an existing UDS when  
156 subject to a wide range of structural failure scenarios involving random cumulative link  
157 failure. Structural failure in an UDS can be modelled by removal of components for example  
158 sewers (links), storage tanks or pumps in the system to represent the inability of the removed  
159 component to deliver its prescribed function. In this study, links in an UDS are randomly and  
160 cumulatively failed and the resulting impacts on the global performance of the system are  
161 investigated for each failure level, until all the links in the system have been failed. This  
162 process of cumulative link failure is used to represent structural failure modes such as sewer  
163 collapse, blockages and sediment deposition in closed systems and blockage resulting from  
164 deposition of solid waste and washed-in sediments in open channel systems. The approach of



165 failing links randomly ensures that all links,  $N$  in the system have an equal probability of  
166 being removed (Johansson and Hassel, 2012). In addition, a step by step increase in sewer  
167 failure levels enables the exploration of the full sewer failure scenario space that ranges from  
168 *predictable* or commonly occurring failure scenarios such as single component ( $N-1$ ), or two  
169 component ( $N-2$ ) failure modes but also other *unexpected* scenarios involving simultaneous  
170 failure of a large number of components (e.g. Johansson, 2010; Park et al., 2013).

171 To fully explore the extent of the failure scenario space in global resilience analysis, a very  
172 large number of model of simulations involving different failure scenarios would be required  
173 to capture the resulting flooding impacts (e.g. Kellagher et al., 2009). In addition, different  
174 possible sewer (link) states for example non-failed (good condition), partial or complete  
175 failure need to be evaluated (Ana and Bauwens, 2010; Kellagher et al., 2009). Taking an  
176 UDS with 81 links as an example, and assuming only two link states (non-failed or  
177 completely failed), the total number of link failure scenarios within the full failure scenario  
178 space would be  $2.4 \times 10^{24}$ . To reduce the computational time, a convergence analysis (e.g.  
179 Trelea, 2003) is carried out to determine the minimum number of random cumulative link  
180 failure sequences,  $rs_x$  that are required to achieve consistent results (refer to Supplementary  
181 information section 1.1). Given the significant computational burden of GRA, a simple 1D  
182 approach to modelling of surface flooding (of the minor system) is proposed rather than using  
183 more complex 2D overland flow models (Digman et al., 2014; Maksimović et al., 2009).

## 184 **2.2 GRA implementation**

185 The GRA method is implemented in the MATLAB environment linked to the Storm Water  
186 Management Model, SWMMv.5.1; a physically based discrete time hydrological and  
187 hydraulic model that can be used for single event and continuous simulation of run-off  
188 quantity and quality, primarily built for urban areas (Rossman, 2010). Link failure can be  
189 modelled in SWMM v5.1 by either significantly reducing pipe diameters in the model (e.g.

190 Mugume et al., 2014a) or increasing the Manning's roughness coefficient,  $n$  to a very high  
191 value. In this study, link failure is modelled by increasing the Manning's  $n$  from its initial  
192 (*non-failed*) state value ( $n = 0.020$ ) to a very high value ( $n = 100$ ). The high value of  $n$  was  
193 chosen because it significantly curtails the conveyance of flows in each failed link and hence  
194 enables modelling of *complete failure* of each link.

195 Model simulations are carried out at each randomly generated link failure level and system  
196 performance is quantified using the total flood volume and mean duration of nodal flooding  
197 as key performance indicators. Surface flooding is simply modelled using the ponding option  
198 inbuilt in SWMM which allows exceedance flows to be stored atop of the nodes and to  
199 subsequently re-enter the UDS when the capacity allows (Rossman, 2010). The flooding  
200 extent at each node is modelled using an assumed ponded area of  $7,500 \text{ m}^2$ . Figure 1 further  
201 illustrates the adopted modelling framework. The main steps in implementing the GRA  
202 include:

- 203 a) A simulation is run to assess UDS performance in its initial (*non-failed*) state using  
204 the considered extreme rainfall loading
- 205 b) A randomly selected single link  $c_i : i = 1, 2, 3, \dots, N$ , in the UDS is failed and a  
206 simulation is run using the same extreme rainfall loading. This step represents single  
207 link failure mode and is denoted as  $N-1$ .
- 208 c) Two randomly selected links, in the UDS are failed (denoted as  $N-2$  *failure mode*) and  
209 the simulation is repeated
- 210 d) The procedure is repeated for all  $N-i : i = 1, 2, 3, \dots, N$  failure modes until all the links in  
211 the system have been failed.
- 212 e) The procedure in (a) – (d) is repeated to determine the minimum number of random  
213 failure sequences  $rs_x$  that ensures *convergence* of results. A detailed description of

214 convergence analysis in GRA is presented in the Supplementary information section  
215 1.1).

216 f) Using the determined  $rs_x$ , the procedure in (a) – (d) above is repeated to investigate  
217 the effect of the proposed adaptation strategies on minimising the loss of system  
218 functionality resulting from the considered cumulative link failure scenarios.

### 219 **2.3 Determination of link failure envelopes**

220 The use of average values in reliability and resilience analysis simplifies results interpretation  
221 but can potentially hide key information about the range of possible failure impacts and  
222 consequences (e.g. Trifunovic, 2012). The process of determining failure envelopes provides  
223 a means of graphically illustrating the range of failure impacts at each considered failure level  
224 (e.g. Church and Scaparra, 2007). In this study, link failure envelopes are determined by  
225 computing the minimum and maximum values of all model solutions (total flood volume and  
226 mean duration of nodal flooding) obtained at each considered link failure level for the  
227 existing UDS and for the considered adaptation strategies. The resulting envelopes represent  
228 the upper and lower limits of the resulting loss of system functionality (impacts) that  
229 therefore provide vital information about the resilience properties of the system being tested.  
230 If the resulting envelope covers solutions with lower impacts at all link failure levels, then the  
231 resulting loss of system functionality is minimised during the considered failure scenarios. If  
232 the resulting envelope covers solutions with higher impacts and with a larger range between  
233 the minimum and maximum values, the tested system exhibits higher loss of system  
234 functionality during the considered failure scenarios (e.g. O’Kelly and Kim, 2007).

### 235 **2.4 Computation of the flood resilience index**

236 The resilience index,  $Res_o$ , is used to link the resulting loss of functionality to the system’s  
237 residual functionality and hence the level of resilience at each link failure level. The resulting  
238 loss of system functionality is estimated using the concept of *severity*,  $Sev_i$  (Hwang et al.,

239 2015; Lansey, 2012). Severity is interpreted as a function of maximum failure magnitude  
 240 (peak severity) and failure duration (Figure 2). Figure 2 illustrates the theoretical response of  
 241 an UDS (in which one or more links have been failed) to a single extreme rainfall loading  
 242 scenario. In Figure 2, severity can be estimated as the (shaded) area between the original  
 243 system performance level,  $P_o$  and the actual system performance curve,  $P_i(t)$ , at any time  $t$   
 244 after occurrence of a given threat that lead to system failure (Equation 1).

$$245 \quad Sev_i = f[Sev_p, t_f] = \frac{1}{P_o} \int_{t_o}^{t_n} (P_o - P_i(t)) dt \quad (1)$$

246 Where  $t_f$  is the failure duration,  $t_o$  the time of occurrence of the threat, and  $t_n$  the total elapse  
 247 time. Equation 1 above is further simplified by assuming that the system failure and recovery  
 248 curve is rectangular (Equation 2)

$$249 \quad Sev_i = \frac{V_{TF}}{V_{TI}} \times \frac{t_r - t_{fs}}{t_n - t_o} = \frac{V_{TF}}{V_{TI}} \times \frac{t_f}{t_n} \quad (2)$$

250 The resilience index,  $Res_o$ , which is a measure of system residual functionality, is estimated  
 251 as one minus the computed volumetric severity and is computed at each link failure level  
 252 (Equation 3).

$$253 \quad Res_o = 1 - Sev_i = 1 - \frac{V_{TF}}{V_{TI}} \times \frac{t_f}{t_n} \quad (3)$$

254 Where  $V_{TF}$  is the total flood volume,  $V_{TI}$  the total inflow into the system,  $t_f$  the mean duration  
 255 of nodal flooding and  $t_n$  the total elapsed (simulation) time.

256 For a given threat (i.e. percentage of failed links), the proposed index quantifies the residual  
 257 functionality of the UDS as function of both the failure magnitude (total flood volume) and  
 258 duration (mean nodal flood duration).  $Res_o$  ranges from 0 to 1; with 0 indicating the lowest  
 259 level of resilience and 1 the highest level resilience to the considered link failure scenarios.  
 260 Resilience envelopes are then derived by plotting the minimum and maximum values of  $Res_o$   
 261 computed at each failure against the percentage of failed links. The resulting envelopes

262 graphically illustrate the system residual functionality at each considered link failure level. A  
263 detailed description the theoretical behaviour of an UDS during failure conditions and the  
264 derivation of the  $Res_o$  is provided in Supplementary information section 1.3.

### 3. Urban drainage system description and modelling results

#### 265 3.1 Case study UDS

266 A case study of the existing urban drainage system in the Nakivubo catchment, a highly  
267 urbanized part of Kampala city, Uganda is used in this work. The system requires  
268 rehabilitation to minimize the frequency, magnitude and duration of flooding during extreme  
269 convective rainfall events (Sliuzas et al., 2013). A model of the existing system is built in  
270 SWMMv5.1. The full dynamic wave model in SWMM is used to route flows through the  
271 modelled UDS. The data needed to build the model has been obtained from a Digital  
272 Elevation Model (DEM) for Kampala (2 m horizontal resolution), a 2011 satellite image for  
273 Kampala (0.5m horizontal resolution), as-built drawings and from existing reports (e.g.  
274 KCC, 2002). A single, non-areally adjusted extreme event was used to represent a worst  
275 functional loading case in the GRA. This event used was recorded on 25<sup>th</sup> June 2012 at 10  
276 minute resolution with a 100 minute duration and depth of 66.2 mm (Sliuzas et al., 2013).

277 The existing primary and secondary conveyance system consists of trapezoidal open channel  
278 sections constructed using reinforced concrete in upstream sections and gabion walls in the  
279 downstream sections. The resulting hydraulic model of the system consists of 81 links, 81  
280 nodes and 1 outfall, and with a total conduit length of 22,782 m. The system drains into the  
281 Nakivubo wetland and finally into Lake Victoria. The gradients of the open channel sections  
282 range from 0.001 to 0.0124. The modelled system drains a total area of 2,793 hectares  
283 delineated into 31 sub-catchments (Figure 3 [Error! Reference source not found.](#)). The  
284 computed average sub catchment slopes and percentage imperviousness range from 0.034 –

285 0.172 (Figure A.1) and 52.3 – 85.7 (Table A.1) respectively. The existing system is not  
286 always clean in a ‘business as usual’ case. This was reflected in the SWMM model by taking  
287 the initial value of *Manning’s n* as 0.020 which is the upper limit of the recommended range  
288 (i.e. 0.010 – 0.020) for concrete lined channels.

### 289 **3.2 Modelling the effect of adaptation strategies on UDS performance**

290 Enhancing the resilience of an UDS during design or retrofit can be achieved by altering its  
291 configuration in order to enhance its redundancy and flexibility. **Redundancy** could be  
292 increased by introducing extra elements such additional storage tanks, temporary storage  
293 areas or increasing spare capacity in critical links (Butler and Davies, 2011; Cabinet Office,  
294 2011; CIRIA, 2014). **Flexibility** on the other hand can be increased, for example, by  
295 designing in future proofing options, use of distributed elements and provision of back-up  
296 capacity (e.g. Gersonius et al., 2013). In this study, two adaptation strategies are modelled  
297 tested using the GRA methodology namely, addition of one large centralised detention pond  
298 (*centralised storage strategy*) and several, spatially distributed storage tanks (*distributed*  
299 *storage strategy*) respectively (Figure A.2).

300 In the *centralised storage* (CS) strategy, a large centralised detention pond with a total  
301 storage volume of  $3.15 \times 10^5 \text{ m}^3$  is introduced upstream of link C47 (Figure A.2a) to enhance  
302 system redundancy. In choosing the possible location of the centralised storage tank, two  
303 main criteria were used; land availability and flow rates in the downstream links in the  
304 primary Nakivubo channel. In the *distributed storage* (DS) strategy, 28 spatially distributed  
305 upstream storage tanks with a combined total storage volume of  $3.15 \times 10^5 \text{ m}^3$  are introduced  
306 at the outlets of the sub catchments to enhance flexibility in crucial points in the network  
307 (Figure A.2b). The DS strategy models upstream distributed source control.

### 308 **3.3 Simulation and performance assessment of the existing UDS**

309 In order to test the performance of the modelled existing UDS, simulations were carried out  
310 and flows were investigated at selected links in the system (Figure 4). The hydraulic data on  
311 the selected open channel cross sections is presented in Table A.2.

312 Lower peak flow rates, are simulated in most upstream links. The flow rates increase along  
313 the system leading to very high peaks in downstream links, for example flows of 297.4 m<sup>3</sup>/s  
314 and 318.2 m<sup>3</sup>/s are simulated at downstream links C76 and C81 respectively after an elapsed  
315 time of 75 minutes (Figure A.3). Globally, 57 links (70.4%) in the system experience  
316 hydraulic overloading that consequently leads to surface flooding. Hydraulic overloading in  
317 links occurs when: (i) the upstream ends of the link run at full capacity and (ii) when the  
318 slope of the hydraulic grade line exceeds the slope of the link (Butler and Davies, 2011). The  
319 most severe hydraulic overloading is simulated in 26 links (32%), with the duration of  
320 hydraulic overloading ranging from 13 – 54 minutes.

321 The results of the simulation also indicate the system experiences flooding at a total of 57  
322 nodes, representing a flood extent of 70.7%, with a total volume of flooding of 706, 045 m<sup>3</sup>  
323 and mean nodal flood duration of 48 ± 4 minutes.

### 324 **3.4 Global resilience analysis of the existing UDS**

325 The proposed GRA methodology described in section 2 is applied to characterise the  
326 performance of existing UDS. The overall performance of the system is quantified by  
327 simulating total flood volume and mean duration of flooding resulting from 16,400 link  
328 failure scenarios generated from 200 random link failure sequences (Figure A.4). The  
329 average values of the total flood volume and duration of nodal flooding are computed for all  
330 the considered link failure scenarios and are presented in Figure 5. The GRA results indicate  
331 that failure of just 10% of links leads to a disproportionately large increase of 91% in total  
332 flood volume (Figure 5a). Thereafter, further increase in the percentage of failed links leads  
333 to comparatively small increases in the total flood volume.

334 The situation is very different for nodal flood duration, where results show failure of 10% of  
 335 links leads to just a 6% increase (Figure 5b). Globally, the results indicate that the failure  
 336 duration increases from 41 minutes to 56 minutes representing an increase of 36.2% when all  
 337 the links in the system are failed.

### 338 **3.5 Effect of adaptation strategies on system performance**

339 The GRA methodology is applied to test each of the proposed UDS adaptation strategies. An  
 340 additional 16,400 link failure scenarios are simulated for the CS and DS strategies  
 341 respectively that is, a total of 32,800 generated from a total of 400 random link failure  
 342 sequences (Figure A.4). The effect of the CS strategy is a slight reduction of flood volume  
 343 which occurs at lower link failure levels less than 60% with very little impact on flood  
 344 duration at all failure levels. Globally, it results in a 3.4% reduction of total flood volume and  
 345 a 1.1% increase in mean duration of flooding (Figure 5).

346 On the other hand, the DS strategy results in a significant reduction of 32% total flood  
 347 volume at all considered link failure levels. At link failure levels greater than 20% any  
 348 additional increase in link failure levels leads to minimal increase in total flood volume. The  
 349 strategy also reduces the mean nodal flooding duration from 48 minutes to 35 minutes giving  
 350 a reduction of 27% for all considered link failure scenarios. Table 3 details the key statistics  
 351 of the GRA results for the existing system and for the considered resilience strategies.

352 | **Table 23:** Mean values of GRA analysis results for all considered link failure scenarios. The values in the  
 353 square brackets indicate the reduction range computed by considering 1 standard deviation of the mean.

Strategy	Flood volume ( $\times 10^3 \text{ m}^3$ )			Mean nodal flood duration (hrs)		
	Mean, $\mu$	Standard deviation, $\sigma$	% reduction	Mean, $\mu$	Standard deviation, $\sigma$	% reduction
Existing system	1,457.5	143.6		0.80	0.07	
Centralised storage	1,408.8	183.4	3.3 [1.0 - 5.1]	0.81	0.07	-1.1 [-2.3 - -0.2]
Distributed storage	986.1	96.3	32.3 [29.9 - 34.1]	0.59	0.03	26.8 [25.6 - 28.4]

354



### 355 **3.6 Link failure envelopes**

356 The resulting link failure envelopes which represent the range of model solutions from the  
357 lowest to the highest flooding impacts computed at each link failure level are presented in  
358 Figure 6. For the existing UDS and considering the flood volume, a large range of deviation  
359 between the computed failure envelopes and the mean values (27 – 87%) is observed at lower  
360 link failure levels (<20%). A convergence of both failure envelopes is observed at higher link  
361 failure levels. The results from the nodal flood duration are different, and indicate a narrow  
362 range of deviation (< 26.3%) between resulting failure envelopes and the mean values at all  
363 link failure levels. Rather similar ranges of deviation between the resulting flood volume and  
364 flood duration failure envelopes and the respective mean values are observed for the CS and  
365 DS strategies respectively.

366 In order to evaluate the effectiveness of the considered adaptation strategies, the generated  
367 link failure envelopes are plotted into one graph to map out the failure space common to all  
368 (Figure 7). Comparing the results of the CS strategy to those of the existing system, a slight  
369 downward shift of both the maximum and minimum flood volume failure envelopes is  
370 observed at lower link failure levels (< 40%), which represents the effect of the strategy in  
371 minimising the magnitude of flooding. However, there is no significant effect at higher link  
372 failure levels. Also, the results suggest that the CS strategy has minimal effect on the flood  
373 duration failure envelopes.

374 For the DS strategy, a significant downward shift in the flood volume failure envelope (i.e. a  
375 reduction in the magnitude of flooding) is observed link failure envelope at all cumulative  
376 link failure levels. The strategy also limits the additional increase in flood volume for link  
377 failure levels beyond 33% i.e. a flattening of the flood volume failure envelope is observed at  
378 higher link failure levels. The strategy also shifts the flood duration failure envelopes

379 downwards (i.e. reduces the failure duration) for all considered link failure levels when  
380 compared the existing UDS.

### 381 **3.7 Resilience index**

382 The resilience index ( $Res_o$ ) is computed using Equation 3, for all simulated link failure  
383 scenarios. Based on the computed indices, resilience envelopes which represent the residual  
384 functionality of the whole UDS as a function of both the failure magnitude and duration are  
385 determined by computing the minimum and maximum values of  $Res_o$  at each link failure  
386 level for the existing system for the tested adaptation strategies (Figure 8). To facilitate  
387 comparison of the performance of the tested strategies, an assumed acceptable level of  
388 resilience threshold of 0.7 is plotted on each of the graphs, as an example of the minimum  
389 acceptable flood protection level of service (for example no property flooding) that needs to  
390 be achieved by the considered adaptation strategies.

391 The figure reveals large variations in  $Res_o$  for the existing system and for the tested strategies  
392 at lower link failure levels ( $< 20\%$ ) with a convergence of the results occurring with  
393 increasing link failure levels. For the existing UDS, the computed mean values of  $Res_o$  range  
394 from 0.54 to 0.66. When compared to the resilience threshold, the results indicate that the  
395 existing system crosses this threshold when link failure levels in system exceed 6.2%.

396 Considering the CS strategy, a slight improvement in  $Res_o$  of 1.2 - 2.3% is observed. The  
397 results indicate that resilience index falls below the threshold value when link failure levels  
398 exceed 8.6%. When the distributed storage strategy is considered, higher mean values of  $Res_o$   
399 are computed (0.76 – 0.84). The results also indicate that for the DS strategy, the resilience  
400 threshold is not crossed at all link failure levels. Overall, the DS strategy leads to significant  
401 improvement in the  $Res_o$  of 27.5 – 41.4%.

## 402 **4. Discussion of results**

#### 403 **4.1 Existing system**

404 Considering the existing system, random failure of less than 20% of the links leads to  
405 disproportionately high degradation of system functionality magnitude (i.e. total flood  
406 volume). The disproportionately high loss of system functionality suggests that failure of a  
407 small fraction of links rapidly reduces the global hydraulic conveyance capacity of the  
408 (minor) system. This result is also confirmed by critical component analysis (e.g. Johansson  
409 and Hassel, 2012) involving targeted failure of single (individual) links in the UDS (Refer to  
410 supplementary information section 1.1, Figure S2) This therefore suggests that the existing  
411 UDS exhibits low levels of resilience to sewer failures. This could be attributed to the already  
412 insufficient hydraulic capacity of the system (due to use of an extreme rainstorm for  
413 modelling purposes) but could also be attributed to other key factors such as its dendritic  
414 network topology and limitations of using 1D modelling approach which excludes the  
415 contribution of the major system (i.e. effect of additional redundancies) in conveying surface  
416 flows to downstream parts of the system during extreme events.

417 In contrast to the total flood volume, random cumulative link failure has a limited effect on  
418 mean nodal flood duration. This could be attributed to use of a single short duration rainfall  
419 event for the simulations as opposed to using multiple events. Similarly, this could also be  
420 attributed limitations of using a simplified above ground flood model. By using a simplified  
421 above-ground flood model, surface flooding which occurs in the major system (i.e. overland  
422 flood pathways such as roads, paths or grass ways) during extreme events and which may  
423 also cause substantial damage to property and infrastructure is not considered, which could  
424 also lead to inaccurate estimation of the mean flood duration (e.g. Digman et al., 2014;  
425 Maksimović et al., 2009).

#### 426 **4.2 Effect of adaptation strategies**

427 It is argued that an effective adaptation strategy should result in a downward shift (i.e.  
428 towards the origin) of the failure envelope of the existing system. By doing this, the failure  
429 magnitude and duration is minimised across the considered failure scenarios. The derived  
430 link failure envelopes suggest that CS strategy has a very limited effect on minimising the  
431 total flood volume, with the reduction being achieved at lower link failure levels. More so, no  
432 significant effect on flood duration at all considered link failure levels. As a consequence, the  
433 CS strategy only minimally improves the residual functionality of the existing system during  
434 the considered link failure scenarios. This therefore suggests that sewer failures could  
435 significantly limit the effectiveness of adaptation strategies involving enhancement of  
436 redundancy at a single location in the UDS. This also suggests that other preventive asset  
437 management strategies for example improved cleaning and maintenance practices may be  
438 more effective for resilience enhancement, because they increase spare capacity in the  
439 links themselves and minimise structural failure in existing systems (e.g. Ten Veldhuis, 2010)

440 In contrast the CS strategy, the study results suggest that the DS strategy is more effective in  
441 minimising the resulting loss of functionality at all link failure levels. This could be attributed  
442 to the effect of increased the spatial distribution of control strategies (i.e. smaller  
443 decentralised upstream storage tanks with the same total storage volume as the CS strategy)  
444 results in optimal use of the total storage volume for reduction both the storm water volume  
445 and the inflow rates before entry into UDS. Reducing the stormwater inflows into the system  
446 in turn enables the degraded UDS to continue functioning with minimal impacts. It could also  
447 be due to a reduction in propagation of hydraulic failures from one part of the UDS to  
448 another, which suggests that the DS strategy improves the flexibility properties of the whole  
449 (minor) system. Using this argument, it could be suggested that adaptation strategies that  
450 increase the spatial distribution of control strategies in upstream parts of the catchment for  
451 example implementation of multifunctional (dual-purpose) rainwater harvesting (DeBusk,

452 2013) at a city district or catchment scale could significantly increase the resilience UDSs to  
453 sewer failures.

### 454 **4.3 Outlook**

455 The developed global resilience analysis approach presents a promising quantitative tool  
456 which opens up new opportunities for holistic and systematic evaluation of the effect of a  
457 wide range of threats that have not been considered in conventional hydraulic reliability  
458 based urban drainage design and rehabilitation approaches. Future research will compare the  
459 results obtained by the presented GRA method with those obtained by using dual-drainage  
460 (1D-1D) or 2D rapid flood spreading models (e.g. Blanc et al., 2012; Maksimović et al.,  
461 2009) in GRA to account for the effect of the major system in providing additional system  
462 redundancies during flooding conditions.

463 Additionally, the following areas are recommended for further research.

- 464 • Investigation of the influence of inherent/inbuilt UDS characteristics for example  
465 network structure, network size (number of links), pipe diameters, pipe gradients on  
466 resilience to structural failures.
- 467 • Investigation of the effect of other types of component failures (e.g. pump failures) on  
468 global resilience in UDSs.
- 469 • Investigation of the linkages and interdependences between UDS failure (flooding)  
470 and unexpected failures in interconnected systems such as electrical power systems.
- 471 • Further investigation aimed at linking the computed resilience indices to new  
472 resilience-based flood protection level of service standards that are based on  
473 minimisation of the magnitude and duration flooding as opposed to use of design  
474 return periods.

## 5. Conclusions

475 This research has tested and extended the global resilience analysis (GRA) methodology to  
476 systematically evaluate UDS system resilience to random cumulative link (sewer) failure.  
477 The GRA method presents a new and promising approach for performance evaluation of  
478 UDSs that shifts emphasis from prediction of the probability of occurrence of key threats that  
479 lead to flooding (fail-safe approach) to evaluating the effects of a wide range of failure  
480 scenarios that not only includes functional failures but also structural or component failures  
481 which also contribute to flooding in cities.

482 In this study, the effect of a wide range of random and progressive sewer (link) failure  
483 scenarios on the ability of existing and adapted UDSs to minimise the resulting loss of  
484 functionality has been investigated. Link failure envelopes have been determined by  
485 computing the minimum and maximum values of the total flood volume and mean nodal  
486 flood duration results generated by simulating a large number of random cumulative link  
487 failure scenarios. A new resilience index has been developed and used to link the resulting  
488 loss of functionality to the system's residual functionality at each link failure level. Based on  
489 the results of the study, the following conclusions are drawn.

- 490 • The presented global resilience analysis approach provides a promising quantitative  
491 evaluation tool that enables consideration of wide range of possible sewer failure  
492 scenarios ranging from *normal* to *unexpected* with reduced computational complexity.
- 493 • The use of convergence analysis enables determination of the minimum number of  
494 random cumulative link failure sequences require to achieve consistent GRA results,  
495 which in turn enhances that practicability of resilience assessment by significantly  
496 reducing the computational complexity involved in simulating all possible sewer  
497 failure combinations.

- 498       • Building resilience in UDSs to unexpected failures necessitates explicit consideration  
499       of the contribution of different failure modes, effect of interactions between different  
500       failures modes for example interdependences between sewer failures and hydraulic  
501       overloading in UDS design or performance evaluation of existing systems.
- 502       • Building resilience in UDSs should not only be addressed through capital investments  
503       aimed at enhancing inherent UDS properties such as redundancy and flexibility but  
504       should also consider investments in asset management strategies such as sewer  
505       cleaning and maintenance of existing UDSs.

### **Acknowledgement**

506 This research is financially supported through a UK Commonwealth PhD scholarship  
507 awarded to the first author. The work is also supported through the UK Engineering &  
508 Physical Sciences Research Council (EPSRC) funded Safe & SuRe research fellowship  
509 (EP/K006924/1) awarded to last author. Acknowledgement is given to the National Water  
510 and Sewerage Corporation (NWSC) and the Kampala Capital City Authority (KCCA),  
511 Uganda for providing datasets used in SWMM model development. Thanks are given to Dr.  
512 Richard Sliuzas (University of Twente, Netherlands) for provision of high resolution  
513 rainfall data for Kampala. The insights of the three anonymous reviewers are also gratefully  
514 acknowledged.

515 **References**

- 516 Ana, E. V., Bauwens, W., 2010. Modeling the structural deterioration of urban drainage  
517 pipes: the state-of-the-art in statistical methods. *Urban Water J.* 7, 47–59.  
518 doi:10.1080/15730620903447597
- 519 Atkinson, S., Farmani, R., Memon, F.A., Butler, D., 2014. Reliability indicators for water  
520 distribution system design: Comparison. *Water Resour. Plan. Manag.* 140, 160–168.  
521 doi:10.1061/(ASCE)WR.1943-5452.0000304.
- 522 Blackmore, J.M., Plant, R.A.J., 2008. Risk and Resilience to Enhance Sustainability with  
523 Application to Urban Water Systems. *Water Resour. Plan. Manag.* 134, 224 – 233.
- 524 Blanc, J., Hall, J.W., Roche, N., Dawson, R.J., Cesses, Y., Burton, A., Kilsby, C.G., 2012.  
525 Enhanced efficiency of pluvial flood risk estimation in urban areas using spatial –  
526 temporal rainfall simulations. *Flood risk Manag.* 5, 143–152. doi:10.1111/j.1753-  
527 318X.2012.01135.x
- 528 Butler, D., Davies, J.W., 2011. *Urban Drainage*, 3rd ed. Spon Press, Taylor and Francis  
529 Group, London and New York.
- 530 Butler, D., Farmani, R., Fu, G., Ward, S., Diao, K., Astaraie-Imani, M., 2014. A new  
531 approach to urban water management: Safe and SuRe, in: 16th Water Distribution  
532 System Analysis Conference, WDSA2014 - Urban Water Hydroinformatics and  
533 Strategic Planning. *Procedia Engineering*, pp. 347–354. doi:doi:  
534 10.1016/j.proeng.2014.11.198
- 535 Cabinet Office, 2011. *Keeping the country running: Natural hazards and infrastructure.*  
536 London.
- 537 Church, R., Scaparra, P.M., 2007. Analysis of facility systems' reliability when subject to  
538 attack or a natural disaster, in: Murray, A.T., Grubestic, T.H. (Eds.), *Critical*  
539 *Infrastructure: Reliability and Resilience.* Springer-Verlag Berlin Heidelberg, pp. 221–  
540 241.
- 541 CIRIA, 2014. *Managing urban flooding from heavy rainfall - encouraging the uptake of*  
542 *designing for exceedance.* London.
- 543 DeBusk, K.M., 2013. *Rainwater Harvesting: Integrating Water Conservation and Stormwater*  
544 *Management.* North Carolina State University, Raleigh, North Carolina.
- 545 Digman, C.J., Anderson, N., Rhodes, G., Balmforth, D.J., Kenney, S., 2014. Realising the  
546 benefits of integrated urban drainage models. *Water Manag.* 167, 30–37.  
547 doi:10.1680/wama.12.00083
- 548 Djordjević, S., Butler, D., Gourbesville, P., Mark, O., Pasche, E., 2011. New policies to deal  
549 with climate change and other drivers impacting on resilience to flooding in urban areas:  
550 the CORFU approach. *Environ. Sci. Policy* 14, 864–873.  
551 doi:10.1016/j.envsci.2011.05.008



- 552 Egger, C., Scheidegger, A., Reichert, P., Maurer, M., 2013. Sewer deterioration modeling  
553 with condition data lacking historical records. *Water Res.* 47, 6762–6779.  
554 doi:10.1016/j.watres.2013.09.010
- 555 Gersonius, B., Ashley, R., Pathirana, A., Zevenbergen, C., 2013. Climate change uncertainty:  
556 building flexibility into water and flood risk infrastructure. *Clim. Chang.* 116, 411–423.  
557 doi:10.1007/s10584-012-0494-5
- 558 Hassler, U., Kohler, N., 2014. Resilience in the built environment. *Build. Res. Inf.* 42, 119–  
559 129. doi:10.1080/09613218.2014.873593
- 560 Holling, C.S., 1996. Engineering Resilience versus Ecological Resilience, in: Schulze, P.  
561 (Ed.), *Engineering within Ecological Constraints*. National Academy Press, Washington  
562 DC, USA, pp. 31–44.
- 563 Hwang, H., Lansey, K., Quintanar, D.R., 2015. Resilience-based failure mode effects and  
564 criticality analysis for regional water supply system. *J. Hydroinformatics* 17, 193–2010.  
565 doi:10.2166/hydro.2014.111
- 566 IPCC, 2014. Summary for Policy Makers, in: Field, C.B., Barros, V.R., Dokken, D.J., Mach,  
567 K.J., Mastrandrea, M.D., Bilir, T.E., Chatterjee, M., Ebi, K.L., Estrada, Y.O., Genova,  
568 R.C., Girma, B., Kissel, E.S., Levy, A.N., MacCracken, S., Mastrandrea, P.R., White,  
569 L.L. (Eds.), *Climate Change 2014: Impacts, Adaptation and Vulnerability -*  
570 *Contributions of the Working Group II to the Fifth Assessment Report*. Cambridge  
571 University Press, Cambridge and New York, pp. 1–32.
- 572 Johansson, J., 2010. Risk and Vulnerability Analysis of Interdependent Technical  
573 Infrastructures Addressing Socio-Technical Systems. PhD Thesis, Lund University,  
574 Lund.
- 575 Johansson, J., Hassel, H., 2012. Modelling, Simulation and Vulnerability Analysis of  
576 Interdependent Technical Infrastructures, in: Hokstad, P., Utne, I.B., Vatn, J. (Eds.),  
577 *Risk and Interdependencies in Critical Infrastructures - A Guideline for Analysis*.  
578 Springer, London Heidelberg New York Dordrecht, pp. 49–65.
- 579 KCC, 2002. Nakivubo channel rehabilitation project, Kampala Drainage Master Plan:  
580 Volume 5 - Inventories. Kampala.
- 581 Kellagher, R.B.B., Cesses, Y., Di Mauro, M., Gouldby, B., 2009. An urban drainage flood  
582 risk procedure - a comprehensive approach, in: *The WaPUG Annual Conference*. HR  
583 Wallingford, Blackpool.
- 584 Lansey, K., 2012. Sustainable, robust, resilient, water distribution systems, in: *14th Water*  
585 *Distribution Systems Analysis Conference*. Engineers Australia, pp. 1–18.
- 586 Maksimović, Č., Prodanović, D., Djordjević, S., Boonya-Aroonnet, S., Leitão, J.P., Allitt, R.,  
587 2009. Overland flow and pathway analysis for modelling of urban pluvial flooding.  
588 *Hydraul. Res.* 47, 512–523. doi:10.3826/jhr.2009.3361

- 589 Mcbain, W., Wilkes, D., Retter, M., 2010. Flood resilience and resistance for critical  
590 infrastructure. London.
- 591 Mugume, S.N., Diao, K., Astaraiie-Imani, M., Fu, G., Farmani, R., Butler, D., 2014. Building  
592 resilience in urban water systems for sustainable cities of the future, in: IWA World  
593 Water Congress and Exhibition. IWA, Lisbon, p. 72.
- 594 O’Kelly, M.E., Kim, H., 2007. Survivability of commercial backbones with peering: A case  
595 study of Korean networks, in: Murray, A.T., Grubestic, T.H. (Eds.), *Critical*  
596 *Infrastructure: Reliability and Resilience*. Springer, Berlin, Heidelberg, New York, pp.  
597 107–127.
- 598 Ofwat, 2012. Resilience - outcomes focused regulation. Principles for resilience planning.  
599 Birmingham.
- 600 Park, J., Seager, T.P., Rao, P.S.C., Convertino, M., Linkov, I., 2013. Integrating risk and  
601 resilience approaches to catastrophe management in engineering systems. *Risk Anal.* 33,  
602 356–367. doi:10.1111/j.1539-6924.2012.01885.x
- 603 Rossman, L., 2010. Storm Water Management Model - User’s Manual Version 5.0.  
604 Cincinnati, Ohio.
- 605 Ryu, J., Butler, D., 2008. Managing sewer flood risk, in: 11th Int. Conference on Urban  
606 Drainage. Edinburgh, Scotland, pp. 1–8.
- 607 Scholz, R.W., Blumer, Y.B., Brand, F.S., 2011. Risk, vulnerability, robustness, and resilience  
608 from a decision-theoretic perspective. *J. Risk Res.* 1–18.  
609 doi:10.1080/13669877.2011.634522
- 610 Sliuzas, R., Jetten, V., Flacke, J., Lwasa, S., Wasige, J., Pettersen, G., 2013. Flood Risk  
611 Assessment, Strategies and Actions for Improving Flood Risk Management in Kampala.  
612 Kampala.
- 613 Sun, S., Djordjević, S., Khu, S., 2011. A general framework for flood risk-based storm sewer  
614 network design. *Urban Water J.* 8, 13–27. doi:10.1080/1573062X.2010.542819
- 615 Ten Veldhuis, J.A.E., 2010. Quantitative risk analysis of urban flooding in lowland areas.  
616 PhD Thesis, Delft University of Technology.
- 617 Thorndahl, S., Willems, P., 2008. Probabilistic modelling of overflow, surcharge and  
618 flooding in urban drainage using the first-order reliability method and parameterization  
619 of local rain series. *Water Res.* 42, 455 – 466.
- 620 Trelea, I.C., 2003. The particle swarm optimization algorithm: Convergence analysis and  
621 parameter selection. *Inf. Process. Lett.* 85, 317–325. doi:10.1016/S0020-0190(02)00447-  
622 7
- 623 Trifunovic, N., 2012. Pattern Recognition For Reliability Assessment Of Water Distribution  
624 Networks. CRC Press. PhD Thesis, Delft University of Technology.

625 Vugrin, E.D., Warren, D.E., Ehlen, M.A., 2011. A resilience assessment framework for  
 626 infrastructure and economic systems: Quantitative and qualitative resilience analysis of  
 627 petrochemical supply chains to a hurricane. Process Saf. Prog. 30. doi:10.1002/prs

628 **Appendix**

629 **Appendix Tables**

630 **Table A.1:** Sub catchment area and computed percentage imperviousness

<b>Sub catchment ID</b>	<b>Sub catchment area (ha)</b>	<b>Imperviousness (%)</b>
S1	83.6	69.9
S2	59.5	71.3
S3	69.0	67.2
S4	97.2	84.1
S5	52.0	81.1
S6	46.1	76.6
S7	23.8	82.7
S8	10.2	66.2
S9	60.0	72.4
S10	144.4	72.0
S11	76.1	71.5
S12	81.4	71.1
S13	50.0	79.6
S14	67.3	75.3
S15	57.4	70.7
S16	55.4	52.3
S17	67.9	61.5
S18	52.9	56.6
S19	52.3	66.7
S20	158.8	61.5
S21	108.5	71.6
S22	71.0	78.2
S23	89.1	82.1
S24	25.4	85.7
S25	199.9	68.1
S26	115.7	62.7
S27	147.5	80.7
S28	134.4	75.8
S29	23.1	81.1
S30	88.7	69.1
S31	424.4	73.0
<b>Total Area</b>	<b>2,793.2</b>	

631

632

633

634

635 **Table A.2:** Hydraulic data of selected trapezoidal open channel sections in the Nakivubo UDS. The slope values  
636 represent ratios of horizontal to vertical distance.

<b>Link</b>	<b>Length (m)</b>	<b>depth, d (m)</b>	<b>bottom width, b (m)</b>	<b>left slope</b>	<b>right slope</b>	<b>Equivalent pipe diameter, D<sub>e</sub> (m)</b>
C12	100.0	1.8	4.3	0.743	0.743	3.5
C40	290.0	2.5	1.0	1.000	1.000	3.3
C54	512.6	1.5	1.0	0.667	0.667	2.0
C76	400.0	4.3	17.4	0.040	0.040	9.8
C81	400.0	2.0	26.0	1.375	1.375	8.6

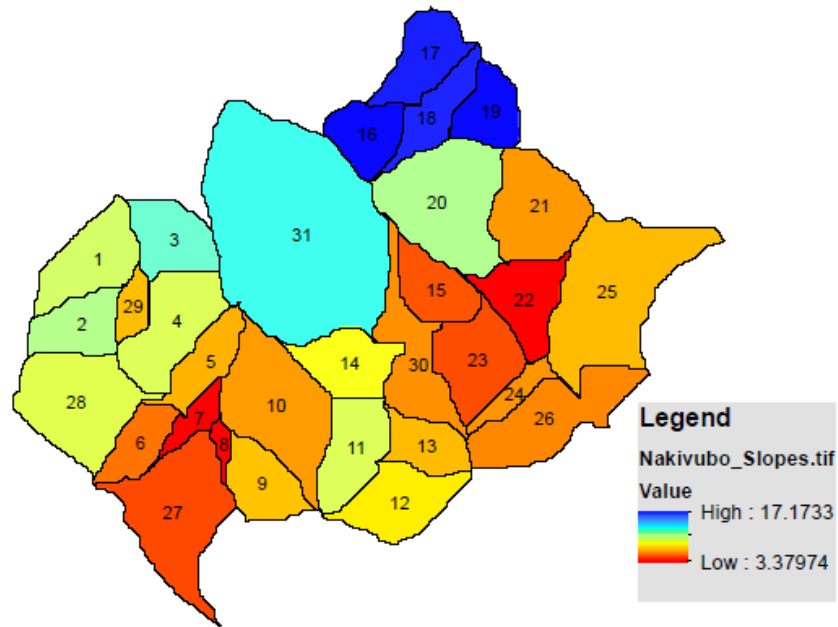
637

638 **Table A.3:** Distributed storage tank volumes

<b>Storage tank ID</b>	<b>Volume (m<sup>3</sup>)</b>
ds1	9,433
ds2	6,711
ds3	7,782
ds4	10,956
ds567	13,743
ds8	1,151
ds9	6,770
ds10	16,287
ds11	8,582
ds12	9,181
ds13	5,639
ds14	7,591
ds16	6,243
ds17	13,623
ds19	5,899
ds20	17,906
ds21	12,239
ds22	8,011
ds23	10,052
ds24	2,859
ds25	22,547
ds26	13,051
ds31	47,864
ds30	10,000
ds29	2,609
ds28	15,160
ds27	16,636
ds15	6,474

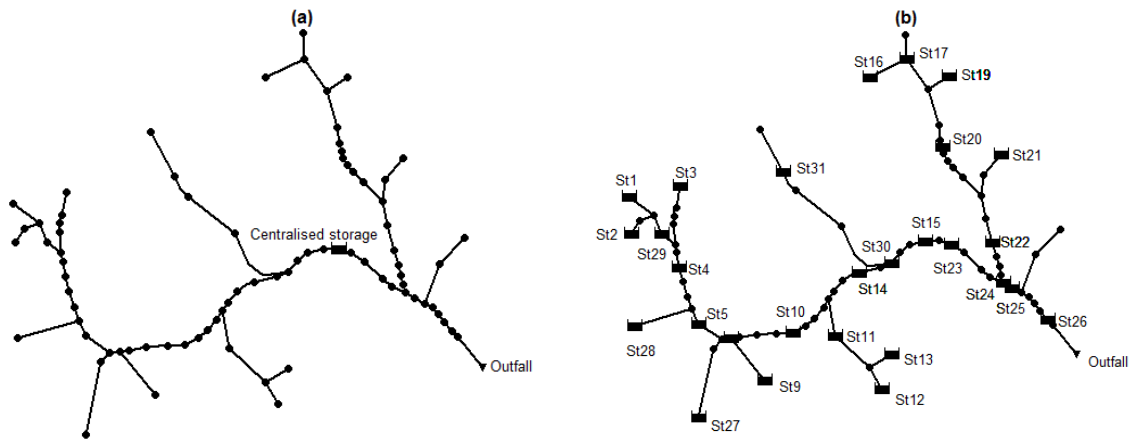
639  
640  
641  
642

**Appendix figures**

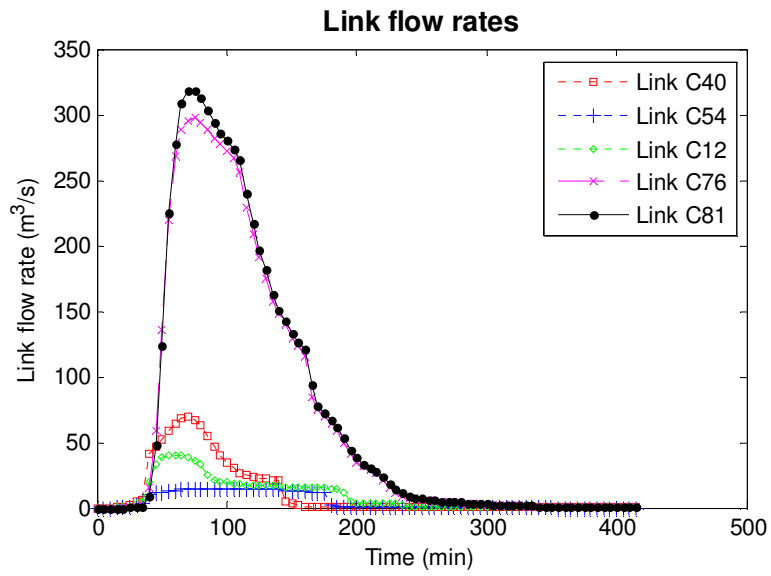


643  
644  
645

**Figure A.1** Computed sub-catchment slopes for the Nakivubo catchment



646 **Figure A.2** Layout of adapted UDS (a) centralised storage strategy (CS) and (b) upstream distributed storage  
647 strategy

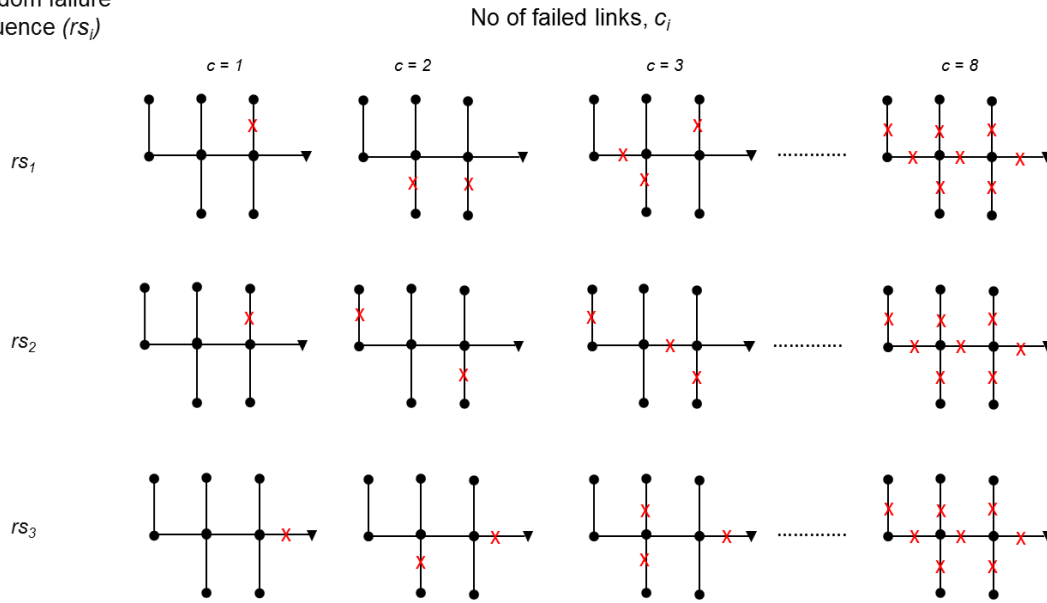


648  
 649  
 650  
 651  
 652  
 653  
 654  
 655

**Figure A.3** Simulated flows in the Nakivubo UDS for upstream links C12, C40, C54 and downstream links C76 and C81.

656 **Figures**

Random failure sequence ( $rs_i$ )

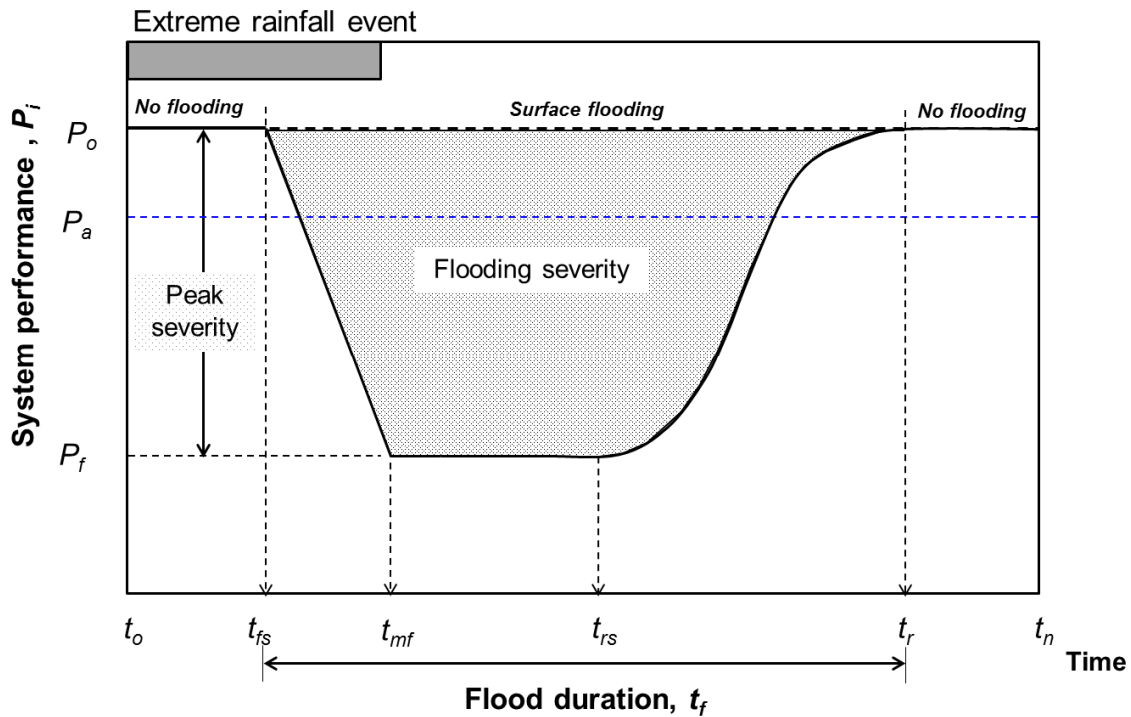


657

658 **Figure 1:** Modelling framework for cumulative link failure in a simplified urban drainage system with 8 links, 8

659 nodes and 1 outflow illustrating (a) increasing link failure levels  $c_1, c_2, c_3, \dots, c_N$  and (b) three potential random

660 failure sequences,  $rs_1, rs_2$  and  $rs_3$ .



661

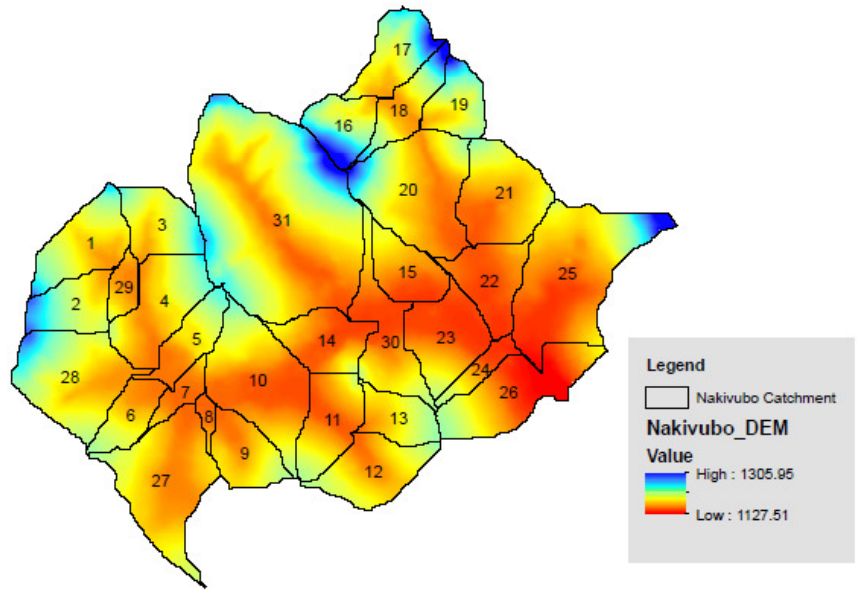
662 **Figure 2:** Theoretical system performance curve for an UDS. The block solid line,  $P_o$  represents the original

663 (design) performance level of service. The blue dotted line,  $P_a$  represents a lower but acceptable level of

664 service.  $P_f$  represents the maximum system failure level resulting from the considered threat.

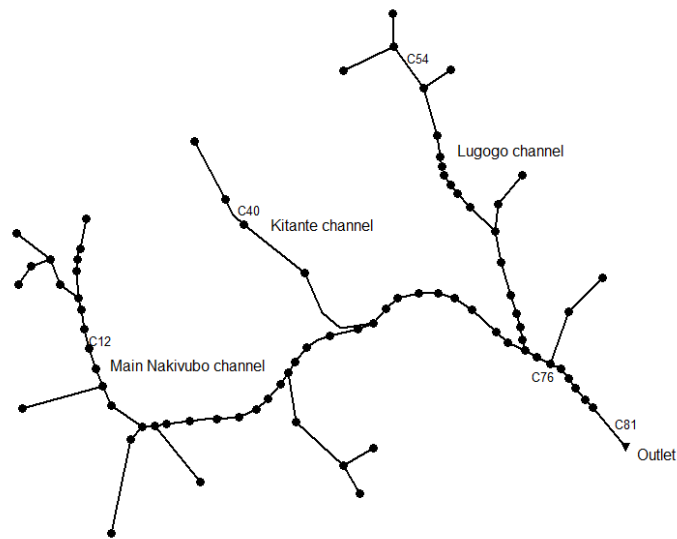
665

666  
667



668  
669  
670  
671

**Figure 3:** Digital elevation model and delineated sub catchments in the Nakivubo catchment

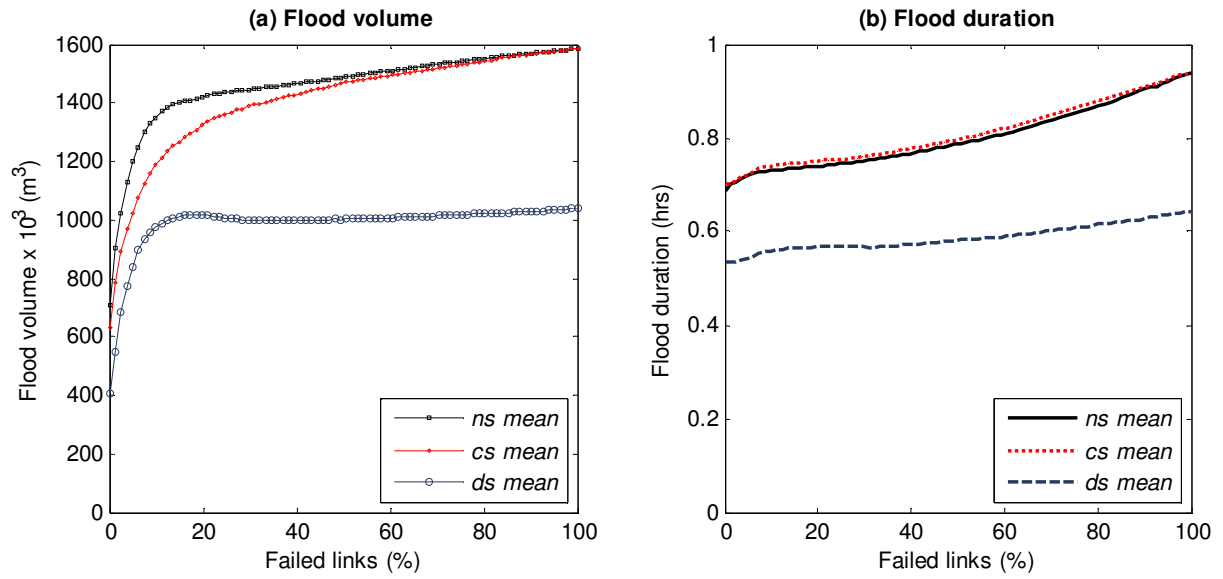


672  
673

**Figure 4:** Layout of the modelled Nakivubo urban drainage network

674  
675  
676



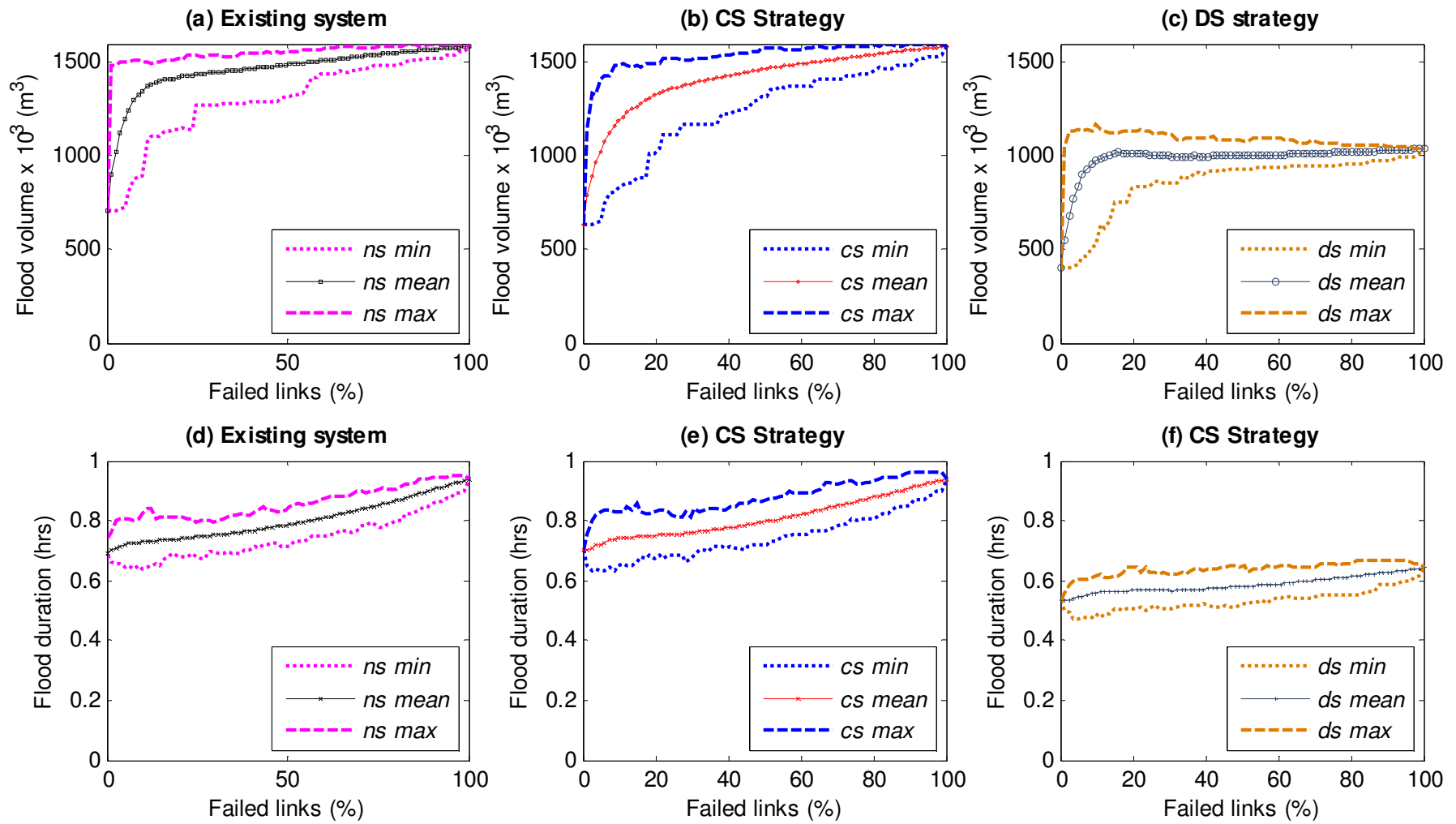


677

678 **Figure 5:** Effect of cumulative pipe failure on (a) total flood volume and (b) mean duration of nodal flooding

679 for the Existing Nakivubo UDS (*ns mean*), for the centralised storage strategy (*cs mean*) and for the distributed

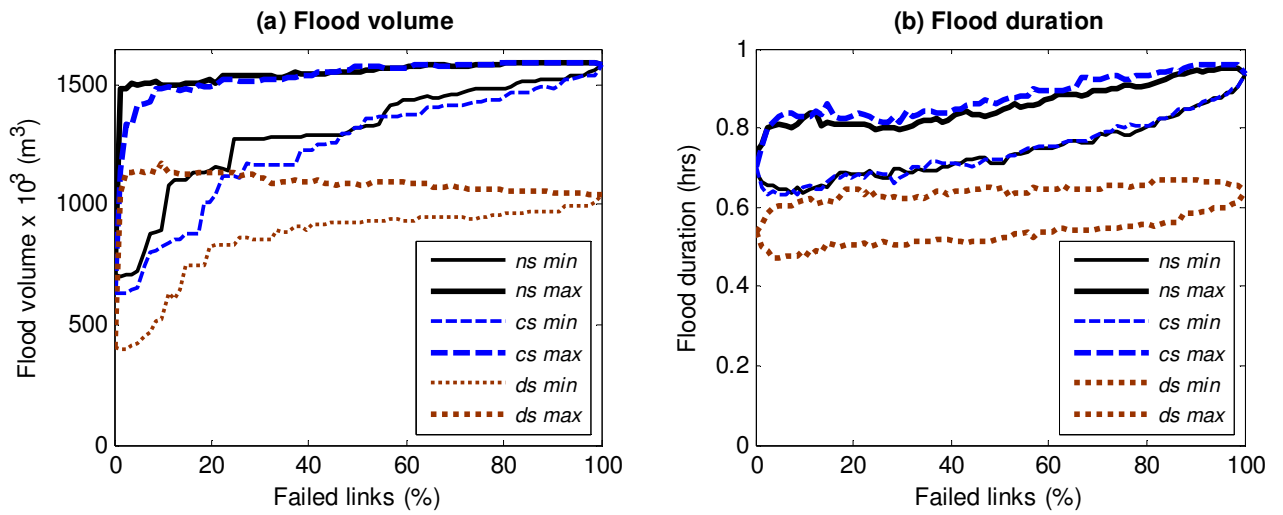
680 storage strategy (*ds mean*).



681

682

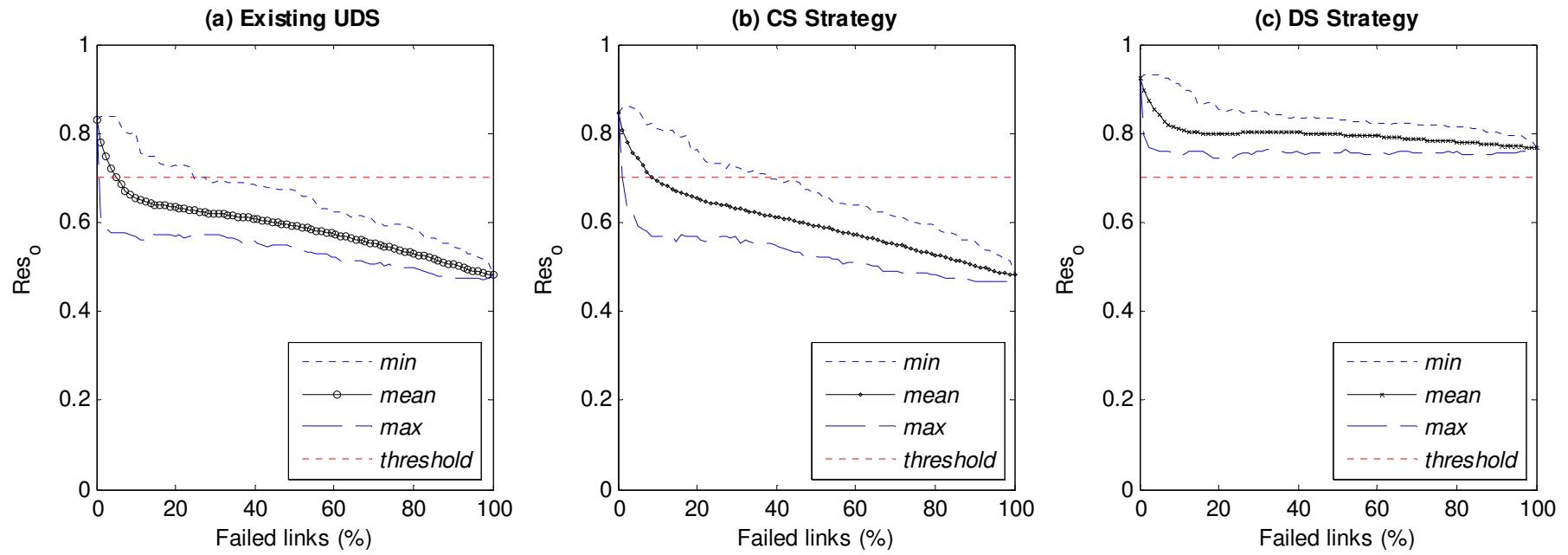
**Figure 6:** Results of the generated link failure envelopes for total flood volume (a) – (c) and for mean duration of nodal flooding (e) – (f)



683  
 684  
 685

**Figure 7:** Intersection of cumulative link failure envelopes for the existing system (*ns min* and *ns max*), CS strategy (*cs min* and *cs max*), and the DS strategy (*ds min* and *ds max*).

686



687

688 **Figure 8:** Resilience envelopes showing maximum, mean, minimum values of  $Res_o$  computed at each link failure level for (a) existing UDS, (b) CS strategy and (c) DS

689 strategy. The red dashed horizontal line is an assumed minimum acceptable resilience level of service threshold of 0.7.

